Materials Today Communications 41 (2024) 110704

Contents lists available at ScienceDirect

Materials Today Communications

journal homepage: www.elsevier.com/locate/mtcomm

Prediction of feed force with machine learning algorithms in boring of AISI P20 plastic mold steel

Aslan Akdulum [a,1,*], Mehmet Süzgünol [b,2], Yunus Kayir [c,3]

[a] Department of Machinery and Metal Technologies, Başkent OSB Vocational School of Technical Sciences, Hacettepe University, Ankara, Turkey
[b] Department of Machine Technologies, Yeşilevler Vocational and Technical High School, Adana, Turkey
[c] Faculty of Technology, Department of Manufacturing Engineering, Gazi University, Ankara, Turkey

ARTICLE INFO

Keywords:
Boring operations
Machine learning models
Process optimization
Feature selection methods
Feature subset detection
Feed force prediction

ABSTRACT

Feed force plays a critical role in machining performance, including efficiency, hole quality, energy consumption, and tool life. While feed force is typically measured using dynamometers, these devices are often impractical in real-world experiments due to their complexity and cost. In particular, boring operations, which are essential for enlarging holes within tight tolerances, depend on precise feed force control to maintain high-quality hole outcomes. Achieving this precision requires reliable pre-process feed force estimation. However, traditional analytical methods for calculating feed force in boring operations often fall short, largely due to factors such as in-hole dynamics, the inclination of the rake surface, and the slenderness of the boring bar. This study aims to apply single and hybrid machine learning methods to accurately model and predict feed force in the boring process. Unlike previous research, which focused on feature selection, we propose the use of all possible combinations of input feature subsets to determine the optimal input features. The results indicate that feed force can be predicted effectively using these optimized feature combinations. Such accurate feed force prediction is crucial for effective process optimization, material selection, and process planning.

1. Introduction

AISI P20 alloy is generally used in plastic injection mold manufacturing [1]. Plastic injection molds are prepared for the rapid and economical production of various plastic-containing products. Because plastic is easier to produce, resistant to corrosion, and chemicals, it is gradually replacing metal in a variety of industries, including shipping, automotive, aerospace, and home appliances [2]. Injection molds are used to create more than 30 % of all plastic parts manufactured [3]. These molds have the capacity to mass produce parts with complex geometry at low cost and within short product cycles. As a result of the massive boost in plastic usage in recent years, the need for injection mold steel has risen dramatically [4]. In the industry, AISI P20 is commonly used in the manufacture of molds and dies with various properties [5]. Molds and dies are manufactured using a variety of machining procedures, including turning, milling, and drilling. Among these machining methods, there is an intense need to produce holes with high quality standards [6]. Machine elements with cylindrical geometry, such as pins and shafts with precise limits and fit tolerance, are inserted into high-quality holes. High hole quality is essential since thousands, hundreds of thousands, or even millions of quality and functional products must be produced from a single mold. The hole quality achieved by various production methods such as casting, extrusion, forging, laser cutting, and flame cutting is often unsuitable for assembly or finishing [7]. To produce high-quality holes, drilling operations with standard drills are not sufficient for a finishing process and may even be more costly due to their solid features [8]. Using the mentioned production methods, hole quality with the desired dimensional accuracy and surface roughness cannot be achieved. Secondary processes are needed to obtain quality holes. Boring heads and boring bars are used to obtain hole quality with high accuracy and precision [9].

Boring bars are cutting tools designed to obtain high hole quality by cutting chips up to the radial cutting depth determined from the inner surface of previously obtained holes, with both feed and rotational

* Corresponding author.
E-mail addresses: a.akdulum@gmail.com (A. Akdulum), mehmetsuzgunol1907@gmail.com (M. Süzgünol), ykayir@gazi.edu.tr (Y. Kayir).
[1] Orcid Id: https://orcid.org/0000-0003-2030-3167
[2] Orcid Id: https://orcid.org/0009-0004-9320-6848
[3] Orcid Id: https://orcid.org/0000-0001-6793-7103

https://doi.org/10.1016/j.mtcomm.2024.110704
Received 8 September 2024; Received in revised form 7 October 2024; Accepted 13 October 2024
Available online 16 October 2024
2352-4928/© 2024 Elsevier Ltd. All rights are reserved, including those for text and data mining, AI training, and similar technologies.

movements along the hole axis [10]. Boring bars are used extensively in various industries. Apart from the molding industry, they are used, for example, in enlarging engine cylinder bores [11]. According to one study, valve seat boring in internal combustion engines occurs around 25 million times each year in Brazil [12]. It has been reported that if the process is not carried out correctly, the sealing of the combustion chamber will be damaged, triggering power loss and increasing harmful gas emissions that adversely affect the environment. These cutters are used in both lathe and milling machines. A lathe is designed to turn the workpiece while keeping the cutting tool fixed. However, in milling machines, the workpiece is stationary, and the cutting tool rotates. Furthermore, in lathe machines, the boring bar has a direct link to the machine's turret. In milling machines, a boring bar is attached to a boring head connected to the spindle, and unlike lathes, centrifugal forces are more effective in cutting tools [13]. These forces may have negative effects on sustainable machining in the drilling process. Additionally, the rigidity of the cutting tool decreases with increasing cutting depth, and chatter problems occur [14]. As a result of unbalanced cutting forces caused by chatter, cutting tools wear out prematurely, and the hole's dimensional accuracy and surface quality deteriorate [15]. This condition necessitates precise planning of boring operations, as it is typically the final step. Any issue in the boring process may result in the molds being scrapped or requiring additional operations. This situation is contrary to the strategy of both efficient use of resources and reducing waste and is extra time-consuming. Therefore, it is very important to determine the optimum input features and output responses. However, when the literature is examined, the number of studies on boring on milling machines is quite limited and insufficient. Research and development studies in this field are a subject that both academia and industry are working on. Specifically, the development of boring heads and boring bars continues with increasing momentum.

One of the most emphasized issues in boring operations is cutting forces, which directly affect hole quality [16]. In addition, cutting forces are examined in detail in order to make inferences about output responses such as power consumption, dimensional accuracy, temperature, chip formation, and surface quality [17]. Apart from this, cutting force is the output response that most directly and effectively reflects the machining state [18]. Modeling and predicting cutting forces in boring operations is a significant area of research. Dynamometers are used to measure real-time cutting forces occurring in boring operations. However, dynamometers, on the other hand, are not appropriate for use in actual experimental conditions due to the need for extra attachments, cables, and data collection. In addition, processing the accumulated data is quite time-consuming and requires specialized expertise. Therefore, the goal is to model cutting forces using alternative methods and estimate them with high accuracy. However, it is difficult to model and calculate parameters such as cutting edge engagement length, chip area, chip flow angle, and cutting edge contact length due to geometric reasons such as inclination angles and chip breakers in the cutting edges used in boring bars [19]. Therefore, low prediction success occurs in the modeling and estimation of cutting force. Accurate modeling and prediction of cutting force and, therefore, feed force are of high importance in terms of process planning, material selection, cutter selection, and optimization of machining parameters.

When the literature is examined, various early studies have been conducted on the modeling and prediction of feed forces. A study on the mechanics of boring operations investigated the variation in chip thickness over the cutting edge as a function of feed rate, depth of cut, nose radius, and tool inclination angle [19]. Modeling was done both analytically and mechanistically, but in some cases, the prediction error was up to 25 %. They attributed this situation to the classical mechanics laws used in boring operations as well as geometric modeling errors. In another study where multi-insert boring bars were mechanically modeled, the prediction error increased to approximately 16 % as the amount of runout increased [20]. Another study developed a thorough time-domain modeling framework to investigate the dynamics of the boring operation [11]. Using this simulation model, while a prediction error of approximately 5 % occurred in chatter-free conditions, the prediction error increased to approximately 90 % in chatter conditions. They demonstrated that the reason for this was an increase in measured forces produced by the combination of the chatter frequency, which was extremely similar to the dynamometer's inherent frequency. In another study, the chip load analytical parametric curve intersection approach was used to analytically and mechanistically model the cutting forces in the boring process [21]. Thus, cutting forces were tried to be predicted by modeling cutting edge contact length, chip flow angle, and chip area. However, prediction deviations of $\pm$ 10 % occurred. In another work, B-spline parametric curves were employed to better represent the cutting edge's nonlinear shape [22]. The dynamics of cutting forces were tried to be modeled analytically, and predictions could be made with a maximum error of 15 %. An attempt was made to develop a cutting-force monitoring system for boring operations [18]. In this system, a system has been developed based on the principle that the strain sensor produces voltage as an alternative to the dynamometer. Cutting forces were determined based on the correlation between voltage and cutting forces. It was determined that the measurement error of the designed system was around 9 %. In another study, the cutting force values obtained by finite element analysis and theoretical calculations were compared, and it was stated that the results were compatible [23]. However, no experimental force measurements were made in the study.

When the literature is examined, the feed force occurring in the boring process has been tried to be estimated by modeling with various methods. Among these methods, mechanical, dynamic, analytical, mechanistic modeling, finite element analysis methods, and strain sensor data were used. Unfortunately, the desired success in precise modeling and prediction of the feed force has not been achieved at a sufficient level. As a result, this topic needs further development and clarification in future investigations. When the reviewed models are examined, finite element analysis and the establishment of mathematical and mechanistic relationships are very time-consuming and labor-intensive processes. In addition, these relationships need to be re-established for each different cutter geometry, workpiece material, and boring parameters. The cutting coefficients required to be used in calculations are quite costly, as they require conducting experiments and comparing the results. Therefore, modeling and forecasting methods with high success rates need to be developed and used. Only advanced methodologies can produce strong and generalizable outcomes. Thus, new modeling and prediction methods need to be researched and developed to precisely model and predict the feed force in the boring process with high accuracy.

Among the new modeling and prediction methods, artificial intelligence-supported methods have gained popularity recently because they enable modeling and prediction with a high success rate. One of the artificial intelligence-supported methods is machine learning algorithms. These algorithms have superior modeling capacity, low calculation time, and very high predictive ability and can be used in embedded systems [24]. Machine learning algorithms have been effectively employed in a variety of areas. Models can be developed to tackle a variety of issues, including regression and classification. Regression techniques are frequently employed for estimating quantitative data, such as feed force. When reviewing the literature, machine learning techniques have been effectively used in earlier research to forecast various output responses produced by the machining process. In a study, the cutting forces that occur during face milling were approximated using random forest (RF), a machine learning technique [25]. In another study, the cutting forces occurring in the turning process were modeled and predicted with the RF algorithm [26]. The adaptive boosting - AdaBoost (AB) algorithm was successfully used to detect chatter occurring in the milling process [27]. The ridge regression (RR) method has been successfully used to predict flank wear in face milling [28]. Tool wear in the milling process was estimated by the categorical gradient boosting - CatBoost (CB) method [29].

It is very important to create datasets by determining input features during the creation of models using machine learning algorithms. There are several methods to select the optimum input features, including processing parameters and data from various sensors. Generally, models are created using more than one dataset. In this way, the model that makes the best prediction is tested and determined [30]. The difference and innovation of this study from previous studies in the literature is that separate datasets are prepared for the combinations of all input features. For example, datasets were obtained by calculating one-feature, two-feature, three-feature, four-feature, and finally five-feature combinations of all boring parameters. The aim here is to determine which input feature combinations can make more successful predictions than others, as the prediction success rate grows with the amount of input features. However, after a certain level, prediction success may decrease, resulting in less successful model predictions [31]. By determining the optimum number of features and feature combinations, quality process planning, the determination of optimal boring parameters, and the prediction of feed force with high accuracy can be achieved.

The purpose of this work is to estimate the feed force in the boring operation of AISI P20 plastic mold steel using machine learning techniques and various boring parameters and combinations. This study uses popular machine learning methods like CatBoost (CB), Random Forest (RF), AdaBoost (AB), and Ridge Regression (RR) to create individual and hybrid models. Performance evaluation indicators were utilized for comparing the established models against one another. The distinctive contributions of the proposed study are presented below.

- While previous studies only included models based on simple analytical equations, the current study proposed the use of innovative artificial intelligence-supported machine learning models to predict the feed force generated in the boring process.
- An indirect measurement method based on optimum input features is proposed to estimate the boring feed force.
- Unlike the feature selection methods of previous research, we propose to use combinations of subsets of all possible input features to determine the optimal input features.
- Hybrid models were established and used in order to obtain more advanced and generalizable results compared to the model successes obtained with individual algorithms.

2. Material and techniques

The research followed the general structure shown in Fig. 1.

2.1. Machine learning

The present research employed machine learning (ML) techniques such as CB, RF, AB, and RR. Additionally, the hybrid architectures listed in Table 1 were generated utilizing the aforementioned algorithms.

Models have been established to forecast feed force using both individual models and hybrid structures. The aforementioned algorithms were used because models with high success rates could be obtained in a short time. Many studies in the literature use these algorithms. Both the input feature and the feed force data are numerical. Therefore, the feed force was estimated using regression techniques. Single algorithms were combined to form hybrid machine-learning models. These hybrid models were generated by averaging the predictions of the individual models. Performance evaluation metrics were created for each established model's ability to predict test results. To create models and make extremely successful predictions using the machine learning method, a training and test set are required. In machine learning algorithms, 70 % of the data, specifically 25 data points, was used for training, and 30 % of the data, specifically 11 data points, was used for testing. To avoid overfitting problems and to establish more generalized models, 5-fold cross-validation was performed. The calculated training and test data were applied for predicting the feed force using the established machine learning algorithms.

2.2. CatBoost - categorical gradient boosting

CatBoost is a type of gradient boosting, a tree-based modeling approach [32]. This method creates a strong learner by sequentially combining many weak predictors. Essentially, it adds new trees by correcting the prediction errors of previous trees. However, CatBoost offers a distinct advantage over other gradient-boosting methods, especially when working with categorical variables [33]. It comes with a specially designed mechanism to automatically deal with categorical variables, reducing users' data preprocessing steps. It contains built-in regularization techniques to reduce overfitting.

2.3. Random forest

Breiman proposed the Random Forest algorithm, which consists of a large number of decision trees [34]. Random forest is a powerful ensemble learning method created by combining many decision trees. Essentially, random sub-datasets are created, and decision trees are trained on each subset. These decision trees make independent predictions using different features and data points. Then, the predictions of these trees are combined to create a single prediction. Random forest can reduce the overfitting problem because the trees are independent and random sub-datasets are generated. Thanks to this feature, it can often be used effectively for regression problems.

2.4. Adaptive boosting – AdaBoost

AdaBoost typically works by sequentially training low-performing models and weighting each model based on its performance [35]. Initially, all data points are assigned equal weight, and an initial weak model is trained. The subsequent model is trained by increasing the weights of misclassified data points. This process enables the creation of successive models, with each model focusing on capturing patterns that previous ones could not. AdaBoost is considered a powerful learning algorithm as each new model focuses on correcting the mistakes of the previous ones, thus improving the overall performance. This technique, which can be used for regression problems, is generally preferred to provide high accuracy and to learn complex data structures.

2.5. Ridge regression

Ridge regression is one of the linear regression methods and is a regularization technique used especially to reduce overfitting and make better generalizations [36]. Essentially, it models the relationship among the independent and dependent features in the same way that classical linear regression does. However, ridge regression works by adding a special regularization term, also known as L2 regularization [37]. This term constrains the coefficients of the model by reducing their magnitude, thereby lessening the tendency for overfitting. Ridge regression can reduce the coefficients of each feature while preserving important features without diminishing the impact of the features that carry the actual signal.

2.6. Cross validation

Cross-validation is an important approach for assessing the performance of machine learning models and determining their generalization abilities. It is mainly used to evaluate how well the model adapts to real-world data in situations where there is a limited amount of data [38]. K-fold cross-validation divides the dataset into random subsets, and the model is trained and validated for each subset. This technique separates the dataset into sections and examines the model's performance on both training and test data [39]. In this way, the misleading results that a

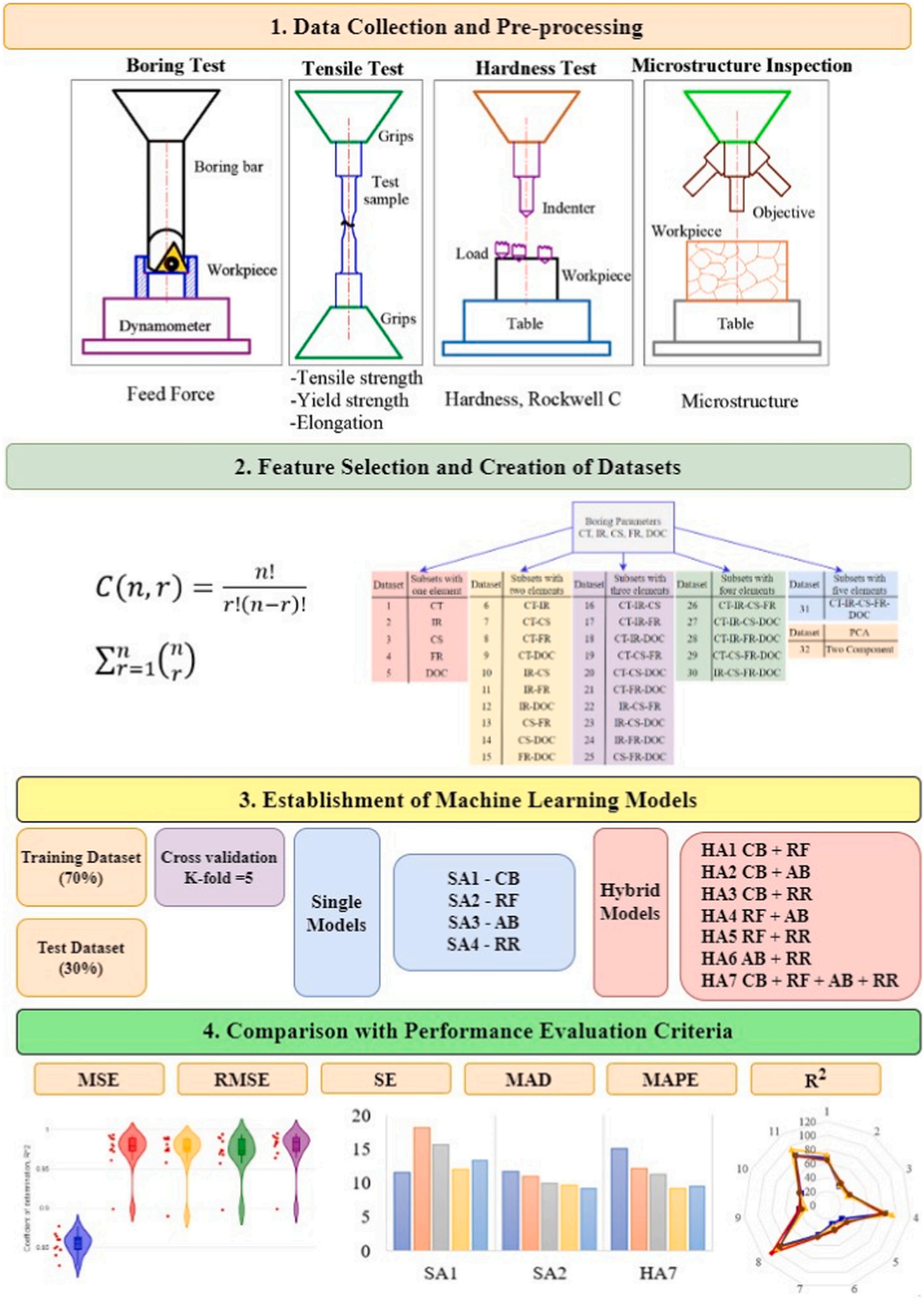


Fig. 1. The general structure for estimating feed force.

Table 1
Hybrid and Single ML algorithms.

Code	Single ML algorithms	Code	Hybrid ML algorithms
SA1	CatBoost - CB	HA1	CB + RF
SA2	Random Forest - RF	HA2	CB + AB
SA3	AdaBoost - AB	HA3	CB + RR
SA4	Ridge Regression - RR	HA4	RF + AB
		HA5	RF + RR
		HA6	AB + RR
		HA7	CB + RF + AB + RR

SA = Single ML algorithms, HA = Hybrid ML algorithms

single training-test split can bring can be avoided. Cross-validation allows for identifying the overfitting tendency of the model, adjusting model parameters, and comparing different model options. In the current study, the K-fold value was determined to be 5.

2.7. Performance evaluation metrics

The training dataset was optimized with the 5-fold cross-validation method. Thirty percent of the dataset was employed for testing, with the remaining 70 % for training. Test predictions and actual test values obtained with the established models were calculated using performance evaluation metrics. This study used metrics such as root mean square error (RMSE), mean absolute error (MAE), mean absolute percentage error (MAPE), mean square error (MSE), standard error (SE), and coefficient of determination (R^2) to compare the models' performance. The reason for choosing many performance evaluation metrics is to successfully compare the feed force predicted by machine learning algorithms with the actual feed force. While lower MSE, RMSE, SE, MAE, and MAPE values are better, it is desired that the R^2 value be closer to 1. Eqs. (1–6) contain formulas for performance evaluation metrics. The number of samples (s), the real values (ri), the estimated values (ki), and the average of real values ($\bar{r}_i$) are represented.

$$MSE = \frac{1}{s}\sum_{i=1}^{s}(r_i - k_i)^2 \tag{1}$$

$$RMSE = \sqrt{\frac{1}{s}\sum_{i=1}^{s}(r_i - k_i)^2} \tag{2}$$

$$SE = \sqrt{\frac{\sum_{i=1}^{s}(r_i - k_i)^2}{s-2}} \tag{3}$$

$$MAE = \frac{1}{s}\sum_{i=1}^{s}|r_i - k_i| \tag{4}$$

$$MAPE = \frac{1}{s}\sum_{i=1}^{s}\frac{|r_i - k_i|}{r_i} \times 100 \tag{5}$$

$$R^2 = 1 - \frac{\sum_{i=1}^{s}(r_i - k_i)^2}{\sum_{i=1}^{s}(r_i - \bar{r}_i)^2} \tag{6}$$

2.8. Experimental installation

The setup for the experiment was designed for estimating the feed force generated during the boring of AISI P20 plastic mold steel on milling machines. A feed force is generated as the boring head and boring bar move along the bore axis, machining the hole in the workpiece. This feed force causes different mechanical and dynamic effects on the boring head and the boring bar. These different effects directly affect the hole quality.

Schematic illustrations of the boring test, tensile test, hardness test, and microstructure examination performed within the scope of the current study are depicted in Fig. 2.

For an experimental study, AISI P20 plastic mold steel material was used with dimensions of 60 × 60 × 35 mm. The chemistry of the workpiece component utilized is shown in Table 2. The mechanical properties obtained because of the tensile test (ASTM E8 / ISO 6892–1) and hardness measurement (ASTM E-18 / ISO 6508) are given in Table 3. The values show the average of tests repeated three times.

The microstructure of AISI P20 material significantly affects its mechanical properties. The workability and hardness of this low-alloy steel can be increased by heat treatment. Grain size, grain boundaries, and phase distribution in the microstructure determine mechanical properties such as tensile strength, hardness, and ductility [40]. While fine-grained structures provide higher tensile strength, the ratio of ferrite and pearlite phases also affects performance. Ferrite provides ductility, while pearlite provides hardness. In addition, defects in the microstructure can negatively affect the load-carrying capacity of the material. Therefore, the microstructural properties of AISI P20 are critical for machining operations. The microstructure (ASTM E112) was visualized with a scanning electron microscope, as shown in Fig. 3. Before boring, the holes were drilled using normal helix drills of different diameters to obtain the appropriate radial depth of cut. Boring, which is a hole-enlargement process, was then carried out from end to end.

Hole boring operations were carried out using a computer-controlled milling machine tool. The workpiece is stationary, while the cutting tool rotates. The machine tool's control panel is Fanuc, with a positioning precision of 0.001 mm. Dandrea brand boring bars, boring heads, and inserts were used. Boring parameters were determined by considering cutting tool catalog recommendations and literature. To measure the feed force, three feed rates (0.04, 0.06, and 0.09 mm/rev), three cutting speeds (130, 162, and 203 m/min), and three radial depths of cuts (0.2, 0.3, and 0.5 mm) were determined. Two types of cermet inserts were used: coated and uncoated. The values of 0.2 and 0.4 were determined as the nose radius of the cutting inserts.

Fig. 4 shows the experimental setup. A Kistler 5070 A amplifier and a Kistler 9272 dynamometer and were used to measure and record the feed force in real time as the hole was enlarged with the boring bar. The Dynoware application was used to process the acquired signal data and determine the average feed force values.

The appropriate boring head and boring bar were used to obtain the 14 mm hole diameter. The boring bar in this range is in class B 3.11 (Ø11-Ø17 mm) in the Dandrea tool set. It has an IT6-grade tolerance. Adjustment precision is 2 microns in diameter. Fig. 5 displays the dimensions of the inserts utilized. Table 4 displays the inserts' geometry and properties. Fig. 6 shows a schematic illustration of the boring bar, insert, and workpiece.

2.9. Data collecting

Machine learning models were developed to predict the feed force values collected during the boring process of plastic mold steels. For this purpose, five input features were determined, as shown in Table 5. The specified input features, or boring parameters, are cutting speed (CS), coating type (CT), insert radius (IR), feed rate (FR), and radial depth of cut (DOC). The input features were employed in numerous studies in the literature to estimate the feed force. The determined parameters have a direct impact on boring operations. However, it has not been clarified to what extent these boring parameters and feature combinations used are effective on the feed force. Increasing the input feature during the establishment of models with machine learning algorithms is important for establishing effective models. However, in some studies, it has been stated that specifying more than a certain number of input features causes the prediction success to decrease.

The goal of this research is to identify the most effective feature

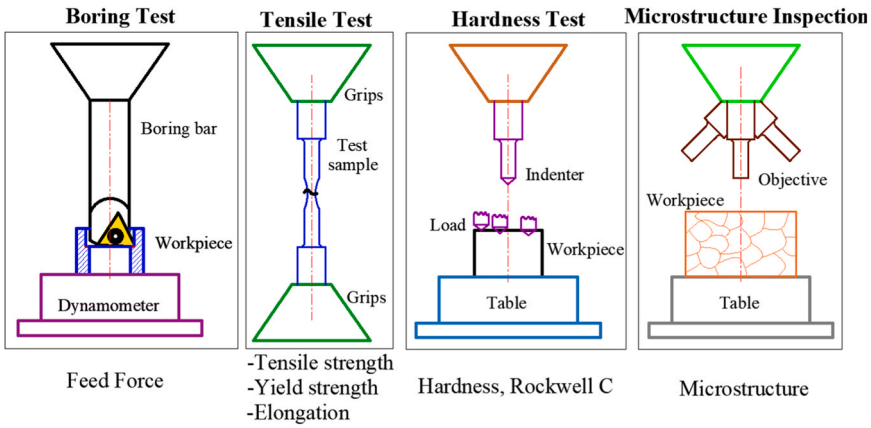


Fig. 2. Schematic illustration of test setups.

Table 2
Chemical composition of AISI P20 plastic mold steel, %.

	Si	Mn	Cr	Mo	C	Fe
AISI P20	0.2	1.5	1.9	0.2	0.4	Balance

Table 3
Measured mechanical properties of plastic mold steel AISI P20.

	Yield strength (Mpa)	Tensile strength (Mpa)	Hardness, Rockwell C (HRC)	Elongation (%)
AISI P20	746	971	35.5	6.2

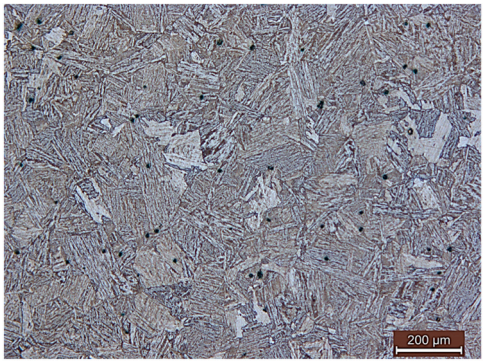


Fig. 3. AISI P20 microstructure image.

combination for achieving the best feed force estimation based on the supplied input attributes. For this purpose, combinations of one feature, two features, three features, four features, and five features were calculated. n represents the total amount of input features, while r represents the number of selected features. For example, when subset combinations with one feature out of a total of five features are calculated, a total of five combinations are formed. The number of subsets with two features is calculated as 10. The number of all combinations for five input features was calculated as 31 according to Eqs. 7 and 8.

$$C(n,r) = \frac{n!}{r!(n-r)!} \tag{7}$$

$$\sum_{r=1}^{n} \binom{n}{r} \tag{8}$$

All calculated combinations were determined separately as input data; thus, the most successful model was tried to be determined. As a result of the calculation, 31 datasets were obtained. Principal component analysis (PCA) was also applied for five input features. PCA is a common technique used to reduce the size of multivariate datasets and express patterns in the data with fewer variables [41]. PCA works by focusing on expressing the essence of the original dataset with fewer components. Another dataset was created in which the two components obtained because of PCA were used as input features. Thus, a total of 32 datasets were obtained. All datasets and input features are shown in Fig. 7. The experimental feed forces were determined by taking an average of the feed forces measured by the dynamometer (Kistler 9272) while boring.

3. Experimental findings and discussion

The goal of the current research is to accurately forecast the boring feed force of AISI P20 plastic mold steel using machine learning algorithms and to identify the optimal combination of input features. The datasets used to estimate the feed force were created by considering all combinations of boring parameters, unlike previous studies in the literature. In different investigations, input features were either used directly or obtained by extracting various features from signals collected during the tests. However, processing the accumulated signal data requires considerable expertise and time. It is difficult to generalize the results for different materials and cutters. Nevertheless, the suggested approach makes it simple to generate a feature matrix and interpret data. A total of 32 datasets created with five features were used to model the feed force and predict it with machine learning algorithms. This approach offers a more efficient and generalizable solution for precise feed force prediction, making it a valuable tool for machining operations.

When the literature is evaluated, different input parameters have an impact on the feed force. Features such as feed rate, cutting depth, and cutting speed that are not optimally selected, especially since the boring bar is slender and long, may cause unstable chatter and lead to deterioration of hole quality [11]. In addition, cutting forces are directly correlated with chip area and chip thickness, but they vary along the tool-chip contact edge due to features such as cutting insert inclination angle, uniform rake surface, chip breaker, nose radius, and depth of cut [19]. This causes variable forces to occur during the cutting process. Variable cutting forces negatively affect machining health and hole quality [42,43]. Therefore, boring parameters must be selected carefully. Fig. 8 shows the interaction between all input parameters and the feed force. Coated inserts have a lower feed force than uncoated inserts because, when compared to the uncoated insert, the coated insert lowers contact friction between the cutter and the material being cut [44]. According to Fig. 8a, increasing the cutting speed decreases the feed

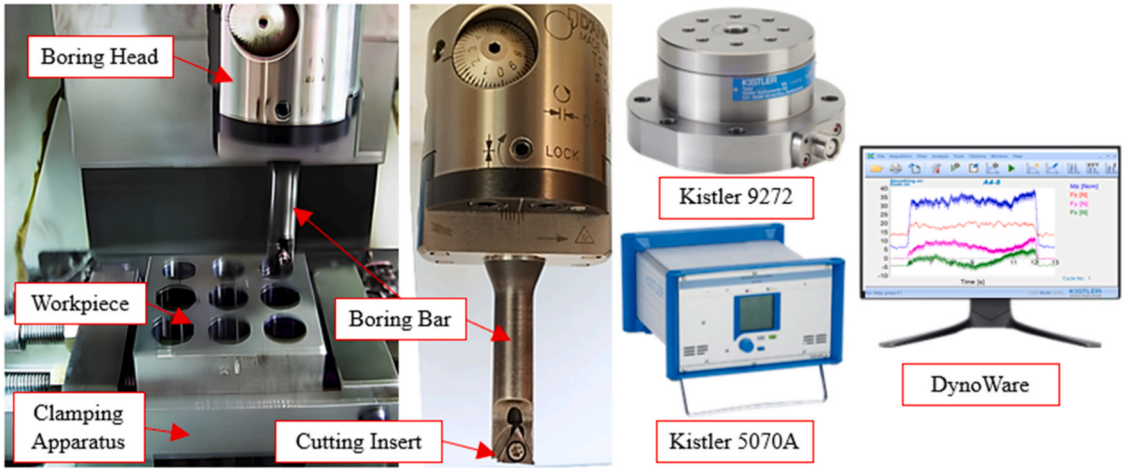


Fig. 4. Experimental setup for feed force measurement.

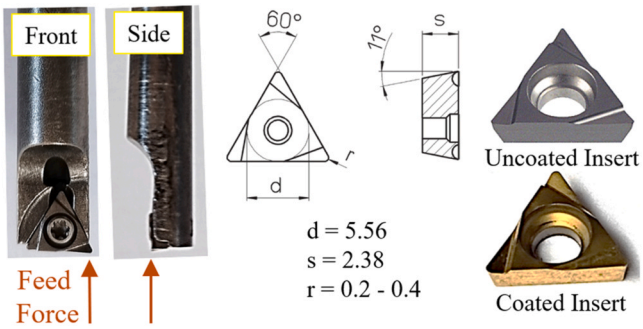


Fig. 5. Boring bar and inserts used.

Table 4
Geometry and properties of the inserts used.

Used insert geometry	Nose radius	Coating	Material
TPGX090202L DC100	0.2	No	Cermet
TPGX090204L DC100	0.4	No	Cermet
TPGX090202L DC100T	0.2	Yes	Cermet
TPGX090204L DC100T	0.4	Yes	Cermet

force, and similar results have been obtained in other studies [45]. The reduction in feed force with cutting speed is related to a decrease in the material's friction coefficient and maximum shear stress at high speeds [11]. Apart from this, it can be said that it is caused by the softening of the workpiece material under higher temperatures, the thinner chips formed with increasing speed, and a reduction in tool-chip friction [46]. In Fig. 8b, extending the radial depth of cut greatly boosts feed force. In terms of the chip area that must be cut per unit time, more effort is necessary to distort the material. In Fig. 8c, a larger insert radius increases the tool-chip engagement length and causes the feed force to increase. In the lathe boring process, the feed force climbed linearly with the feed rate [21]. However, in Fig. 8d, a complex non-linear relationship occurred. This condition can be related to the fact that the cutting depths (0.2–0.3–0.5) chosen to be larger than the cutting nose radius (0.2–0.4) in boring operations done in milling, unlike turning, result in complex interactions between cutting force, depth of cut, tool geometry, and feed rate [11]. However, in the current investigation, a feed force has a linear connection with the depth of cut but a nonlinear relationship with the feed. As a result, the determined boring parameters have effects on the feed force. It is still necessary to determine which combination of parameters is more effective in terms of estimating the feed force. Because larger feed forces can cause more power consumption, poorer surface quality, and higher temperatures, which can reduce tool life [44]. On the other hand, lower feed rate and cutting speed require more time, resulting in increased costs and lower efficiency. Therefore, it is very important to determine the optimum feed forces and, therefore, the optimum boring parameters. In the studies conducted so far, simple analytical relationships have generally been examined for the boring process performed on the milling machine. However, there is a need for methods that can effectively model the complex relationships and patterns between boring parameters by recognizing them. When recent studies are reviewed, artificial intelligence-supported machine learning methods come to the fore. Therefore, modeling and estimating the boring feed force using machine learning algorithms is very important for effective process planning and optimization.

Fig. 9 shows the Pearson correlation coefficients between feed force and input features. A statistical tool for evaluating the linear relationship between two variables is the Pearson correlation coefficient. It can have a value between −1 and 1. −1 denotes a complete negative linear relationship between two variables; 1 indicates a positive linear relationship; and 0 indicates no linear relationship. While the feature with the highest correlation to feed force was the depth of cut, no significant correlation was found with other features. However, investigations have revealed that the distribution of the resulting chip thickness across the cut is nonlinearly related to the radial cutting depth, feed rate, and insert nose radius [11]. Thus, it is crucial to examine these combinations of input features. Artificial intelligence-based methods have shown great success in understanding complex, nonlinear interactions. Machine learning algorithms, one such method, have become very popular recently. ML can make highly successful predictions by supporting the development of effective models. The selection of input features is very important for establishing effective models and estimating the boring feed force with high accuracy, because input features that are not related to the output response can negatively affect the estimation success of the model. Therefore, it is assessed that input features with high correlation with the output response increase the modeling success. In this respect, determining the most optimal input parameter combination by testing the input feature combinations one by one is very important for accurately estimating the boring feed force.

This study employed four individual algorithms for machine learning in modeling and prediction: CatBoost (CB), Random Forest (RF), AdaBoost (AB), and Ridge Regression (RR). These algorithms were chosen because of their fast calculation times and high forecast accuracy. Furthermore, seven hybrid frameworks were created to improve both the forecast accuracy and balance of these four algorithms. Combining hybrid structures and other machine learning techniques that are coupled with or complement one another can result in more powerful

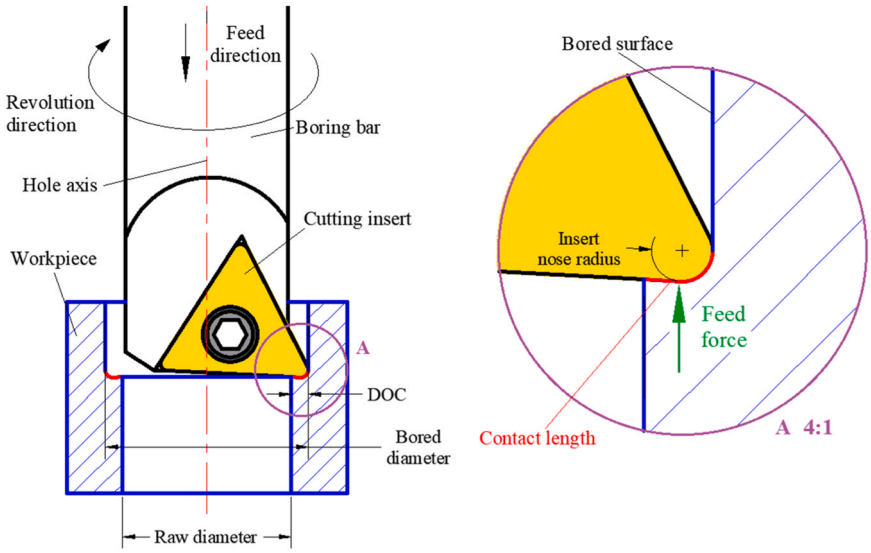


Fig. 6. Schematic illustration of boring bar, insert and workpiece.

Table 5
Input variables and values.

Coating Type CT	Insert Radius IR, mm	Feed Rate FR, mm/rev	Cutting Speed CS, m/min	Radial Depth of Cut DOC, mm
Coated - 1	0.2	0.04	130	0.2
Uncoated - 2	0.4	0.06	162	0.3
		0.09	203	0.5

and efficient models [47]. Making higher generalizations can help to eliminate overfitting concerns [48]. Similar hybrid structures are found in various studies in the literature [24,31]. The findings from the established models were analyzed using six performance evaluation indicators: RMSE, MSE, SE, MAE, MAPE, and R^2. In this study, the goal is to determine the most optimal boring feature combination and estimate the feed force with a high success rate. For this reason, 31 datasets were generated by calculating all combinations of the boring features identified. Furthermore, dimensionality reduction was performed with PCA to correctly predict the feed force. After reducing the data, two components were computed to be assessed with all single and hybrid ML models. The two components generated using PCA account for nearly 99.9 % of the dataset.

When Table 6 is examined, there are coefficients of determination for datasets created with a single feature. According to the table, the maximum coefficient of determination was achieved at 0.973 with the model established for Dataset 5, created with the DOC feature. It was concluded that the high correlation value between DOC and feed force resulted in a high coefficient of determination. Although the correlation coefficient of other input features is low, the obtained coefficients of determination are relatively high. The lowest coefficient of determination value was obtained at 0.836 for the IR feature. Different results were obtained from the various ML algorithms used. For each dataset, different models produced the greatest coefficient of determination score. Only regarding the CT feature did the hybrid model HA7 have the greatest coefficient of determination score. For other features, single algorithms produced higher values. When Fig. 10 is examined, where the models established with one feature are visualized, the greatest coefficients of determination were obtained from the models established with the dataset created with the DOC feature. Models built with the CT feature resulted in very close coefficient of determination values. The success of the models established with one feature aligned with the Pearson correlation coefficient values. There are models in the literature that are established by selecting one feature [24]. Compared to similar studies (R^2 = 0.503–0.624), the coefficients of determination obtained

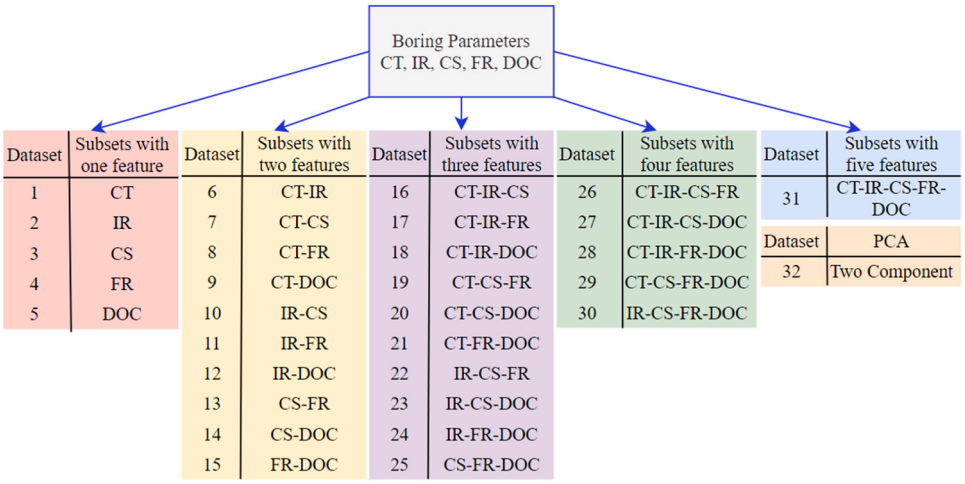


Fig. 7. Datasets and feature combinations.

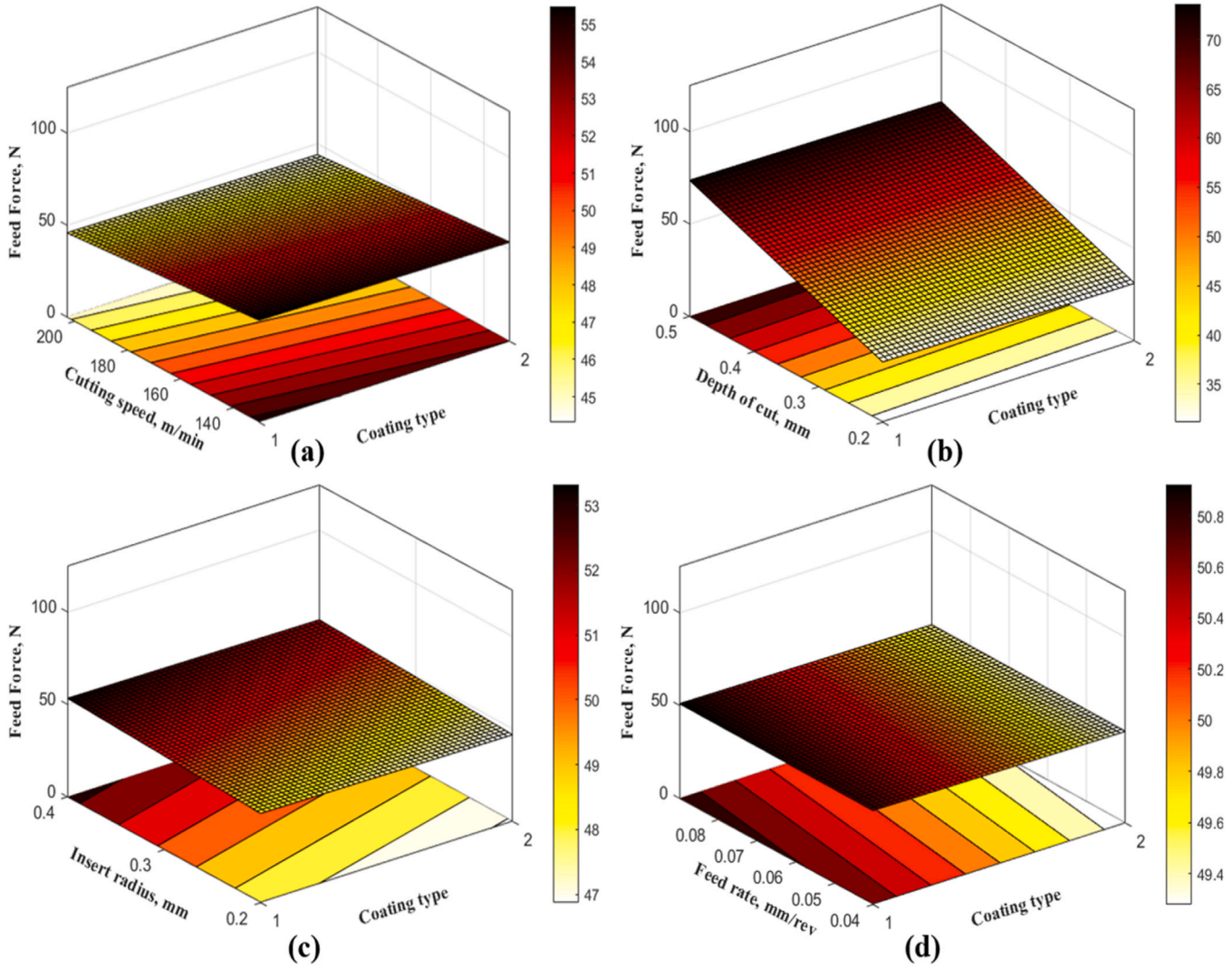


Fig. 8. Interaction of coating type with other boring properties **(a)** IR, **(b)** FR, **(c)** DOC, **(d)** CS.

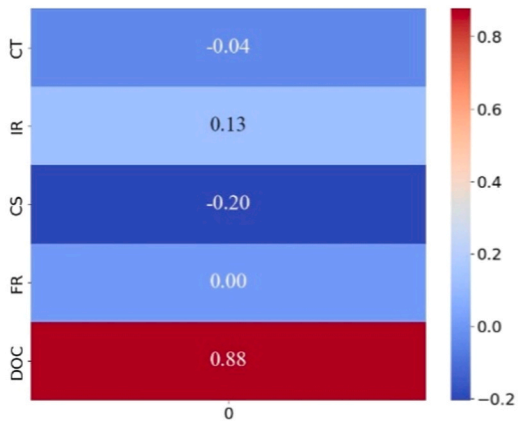


Fig. 9. Pearson correlation coefficients between features and feed force.

in the current study ($R^2 = 0.81–0.973$) were calculated at an acceptable level.

Table 7 shows the coefficients of determination for models built with datasets containing two features. Among the single models, SA4 produced the greatest coefficient of determination for four separate datasets, and SA2 produced the greatest coefficient of determination for three different models. Therefore, the model with the highest performance for the two feature combinations was obtained with SA2, namely random forest. Among the models built with datasets containing two features, the greatest coefficient of determination was achieved with the CS-DOC combination, dataset 14. The coefficients of determination obtained by the models for datasets built using combinations of the DOC feature were higher. The lowest performing models were obtained for CT-IR and CT-FR datasets with SA4, i.e., the ridge regression algorithm. When Fig. 11 is examined, higher coefficients of determination were obtained for all models where the DOC feature was included in the combination. When determining datasets, using features with a high correlation to output responses is very important for creating successful models. Another noteworthy point is that the SA4 algorithm demonstrated a more successful prediction ability among models built with input features with lower correlations. In datasets with high correlations between features, the SA2 method resulted in more successful models and was more effective in making predictions. While the SA3 algorithm produced the greatest coefficient of determination for the CT-DOC dataset, the best performance could not be achieved with the SA1 algorithm. Some of the models created with two features had higher coefficients of determination compared to models created with a single feature. The result is consistent with other research in the literature [31].

Table 8 shows the coefficients of determination for datasets with

Table 6
Models obtained with datasets that have a feature.

R^2		Established machine learning models										
Dataset	**Features**	**SA1**	**SA2**	**SA3**	**SA4**	**HA1**	**HA2**	**HA3**	**HA4**	**HA5**	**HA6**	**HA7**
1	CT	0.837	0.836	0.834	0.837	0.837	0.837	0.837	0.837	0.837	0.837	**0.837**
2	IR	0.836	0.830	0.826	**0.836**	0.833	0.831	0.836	0.828	0.833	0.832	0.832
3	CS	0.810	0.812	**0.880**	0.840	0.811	0.852	0.825	0.853	0.827	0.866	0.841
4	FR	0.836	**0.838**	0.813	0.836	0.837	0.826	0.836	0.828	0.837	0.827	0.832
5	DOC	**0.973**	0.971	0.942	0.889	0.972	0.960	0.943	0.958	0.941	0.924	0.952

Bold: The test datasets' most significant coefficients of determination.

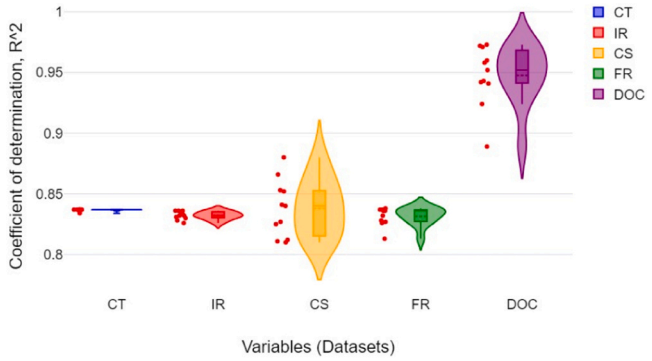


Fig. 10. Coefficients of determination obtained with datasets with a feature.

three features. With SA2, higher coefficients of determination were obtained for more datasets. The lowest values were achieved using the SA4 model. For datasets with three features, datasets 19 and 20 had the highest coefficients of determination. In other words, the most successful models in three-combination models, as in two-combination models, were obtained with the SA2, namely the random forest algorithm. The least successful model was obtained with the CT-FR-IR dataset and the SA4 algorithm. Fig. 12 shows that, unlike combinations with the DOC feature, the coefficient of determination of the model generated with the dataset containing the CT-CS-FR feature combination was relatively high. It is noteworthy that for CT, CS, and FR, the coefficients of determination in one-feature and two-feature combinations resulted in relatively low values, while the triple combination resulted in the highest coefficient of determination. It can be said that features that have a lower impact individually cause a greater impact when combined. Considering only features with high correlation coefficients is not sufficient for effective modeling. Establishing models by creating different combinations of all features is very important and necessary for

Table 7
Models obtained with datasets with two features.

R^2		Established machine learning models										
Datasets	**Features**	**SA1**	**SA2**	**SA3**	**SA4**	**HA1**	**HA2**	**HA3**	**HA4**	**HA5**	**HA6**	**HA7**
6	CT-IR	0.829	0.829	0.826	**0.837**	0.829	0.828	0.835	0.828	0.835	0.833	0.832
7	CT-CS	0.82	0.813	0.805	**0.84**	0.817	0.813	0.833	0.809	0.829	0.826	0.822
8	CT-FR	0.792	0.795	0.783	**0.837**	0.794	0.791	0.82	0.792	0.822	0.813	0.807
9	CT-DOC	0.976	0.974	**0.981**	0.889	0.975	0.979	0.944	0.978	0.943	0.948	0.964
10	IR-CS	0.864	0.875	0.872	0.84	0.87	0.87	0.857	**0.876**	0.863	0.868	0.869
11	IR-FR	0.839	0.835	0.767	0.836	0.837	0.809	**0.842**	0.806	0.84	0.808	0.826
12	IR-DOC	0.984	**0.989**	0.953	0.890	0.987	0.988	0.975	0.985	0.970	0.927	0.981
13	CS-FR	0.752	0.776	0.796	**0.840**	0.765	0.778	0.808	0.789	0.815	0.822	0.799
14	CS-DOC	0.958	**0.990**	0.961	0.898	0.978	0.960	0.982	0.980	0.975	0.986	0.989
15	FR-DOC	0.967	**0.970**	0.963	0.889	0.969	0.967	0.947	0.968	0.946	0.938	0.960

Bold: The test datasets' most significant coefficients of determination.

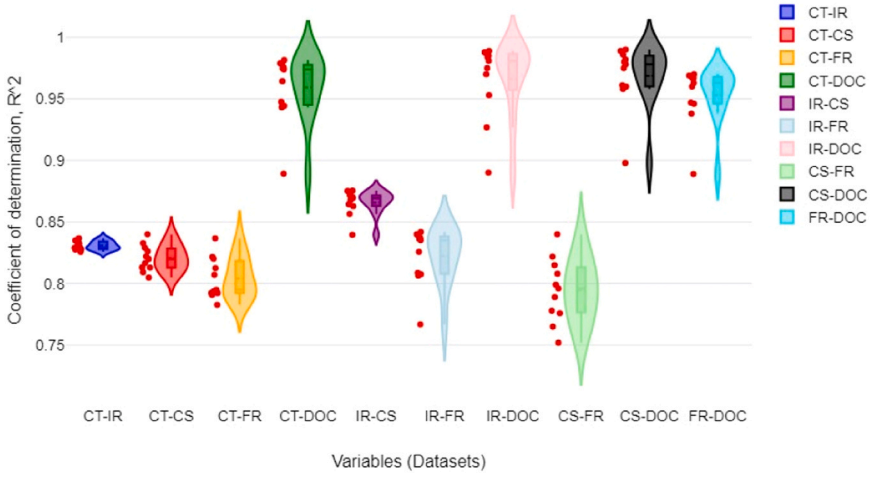


Fig. 11. Coefficients of determination obtained with datasets with two features.

Table 8
Models obtained with datasets with three features.

R^2		Established machine learning models										
Datasets	**Features**	**SA1**	**SA2**	**SA3**	**SA4**	**HA1**	**HA2**	**HA3**	**HA4**	**HA5**	**HA6**	**HA7**
16	CT-IR-CS	0.848	0.876	0.865	0.84	0.873	0.858	0.893	0.881	0.874	**0.9**	0.891
17	CT-IR-FR	0.81	0.808	0.802	**0.837**	0.812	0.81	0.834	0.808	0.828	0.826	0.822
18	CT-IR-DOC	0.97	**0.991**	0.972	0.89	0.985	0.971	0.975	0.986	0.969	0.977	0.988
19	CT-CS-FR	0.968	**0.993**	0.962	0.898	0.987	0.975	0.97	0.984	0.972	0.988	0.991
20	CT-CS-DOC	0.968	**0.993**	0.962	0.898	0.987	0.974	0.97	0.983	0.973	0.986	0.991
21	CT-FR-DOC	0.98	**0.986**	0.974	0.889	0.984	0.979	0.946	0.982	0.953	0.95	0.97
22	IR-CS-FR	0.839	**0.882**	0.848	0.840	0.865	0.846	0.869	0.872	0.875	0.872	0.874
23	IR-CS-DOC	0.960	**0.990**	0.959	0.899	0.979	0.960	0.983	0.978	0.977	0.985	0.990
24	IR-FR-DOC	0.944	0.973	0.933	0.890	0.964	0.945	0.963	0.956	0.975	0.974	**0.977**
25	CS-FR-DOC	0.977	0.989	0.968	0.898	**0.990**	0.980	0.962	0.985	0.978	0.972	0.988

Bold: The test datasets' most significant coefficients of determination.

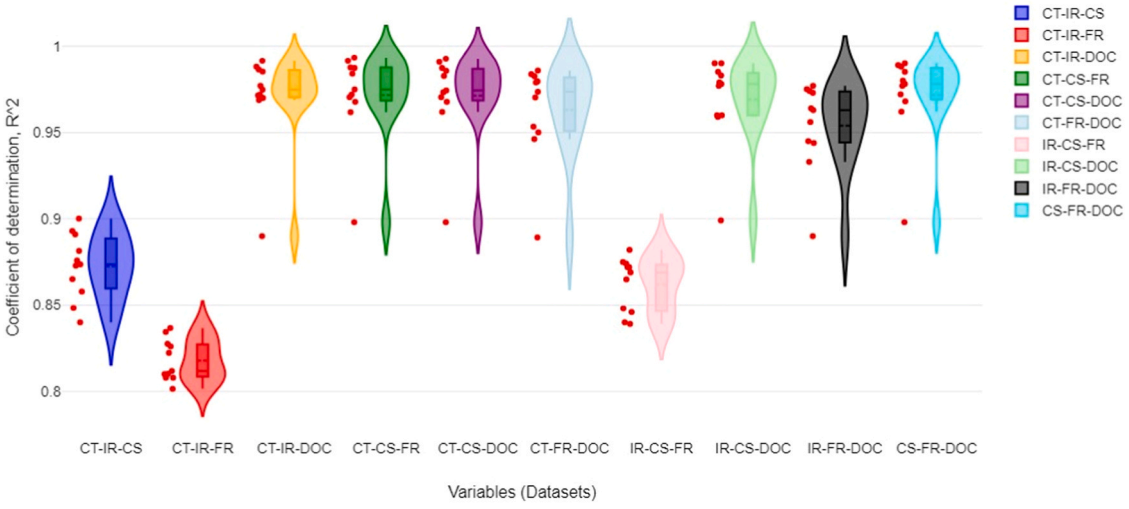


Fig. 12. Coefficients of determination obtained with datasets with three features.

highly successful predictions. While higher coefficients of determination were obtained compared to some studies in which three features were considered [24,31], similar results were obtained in some others [41].

Table 9 and Fig. 13 show the coefficients of determination and their visualizations for the models established with datasets containing four features. The hybrid model HA7 provided the highest coefficient of determination. In addition, the hybrid model HA7 produced the largest coefficient of determination in dataset 27. HA7 is a hybrid model that is calculated by taking the average of the estimates made with all the algorithms used. The limitations of each algorithm, when combined, can provide higher-performance models. In this study, the highest estimation success was achieved with hybrid models. The significant effect of the highly correlated DOC feature was also evident here. The coefficient of determination was calculated as 0.993 with the CT-CS-FR combination in the SA2 model with datasets containing three features. When the IR feature was added to the combination of the three mentioned features, the highest determination coefficient value was 0.877 with the HA3 model. The coefficient of determination was calculated as 0.933 with the model created with CT-CS-DOC. When the IR feature was added to this combination, the same value was calculated for the combination of four features. In other words, it can be said that increasing the number of input features more than necessary does not increase model success and, on the contrary, sometimes decreases it. Therefore, to create effective models, the input dataset and the model diversity to be established are very important. More successful models require the use of a larger number of datasets and algorithms. In addition, all models established with dataset 26 created lower coefficients of determination compared to other datasets. Therefore, the importance of the datasets and the input features to be used in establishing models with higher prediction success is substantial.

When all features from the dataset in Table 10 are incorporated, the models constructed using the hybrid machine learning approach have the highest coefficient of determination. The model's coefficient of determination built from the components obtained when PCA was

Table 9
Models obtained with datasets with four features.

R^2		Established machine learning models										
Data sets	**Features**	**SA1**	**SA2**	**SA3**	**SA4**	**HA1**	**HA2**	**HA3**	**HA4**	**HA5**	**HA6**	**HA7**
26	CT-IR-CS-FR	0.851	0.860	0.827	0.840	0.860	0.847	**0.877**	0.849	0.864	0.860	0.867
27	CT-IR-CS-DOC	0.972	0.992	0.961	0.899	0.988	0.975	0.974	0.981	0.979	0.989	**0.993**
28	CT-IR-FR-DOC	0.974	**0.990**	0.973	0.890	0.989	0.981	0.958	0.988	0.973	0.976	0.988
29	CT-CS-FR-DOC	0.969	**0.994**	0.968	0.898	0.990	0.974	0.957	0.989	0.973	0.972	0.985
30	IR-CS-FR-DOC	0.985	0.989	0.964	0.899	0.992	0.984	0.970	0.979	0.982	0.990	**0.995**

Bold: The test datasets' most significant coefficients of determination.

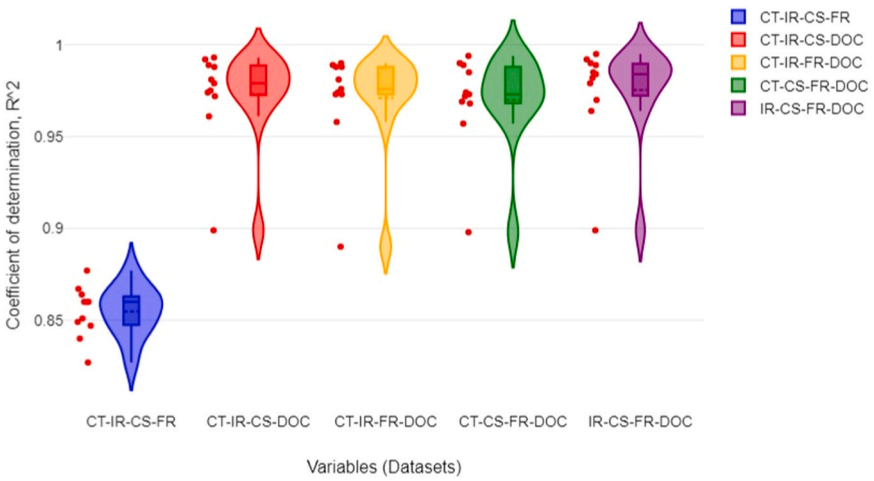


Fig. 13. Coefficients of determination obtained with datasets with four features.

applied to all features was substantially lower. In some studies, it is stated that PCA increases model success by contributing to the creation of an effective model [49]. In some studies, on the contrary, there is a decrease in the coefficients of determination [41]. In the current study, while the coefficient of determination was 0.994 when all features were used, a value of 0.844 was obtained after PCA. PCA did not make a positive contribution to the current dataset, nor did the ML models used. Therefore, using multiple input features together may lead to more complex models or even lower performance.

When Table 11 and Fig. 14 are evaluated, the most successful model determination coefficients are displayed based on the number of features. As the number of features in a dataset grows, so do the coefficients of determination. However, the model with four features yielded the biggest coefficient of determination. Hybrid models tend to perform better as the number of features grows. Hybrid models that included all machine learning approaches outperformed models with four or five features. Different success rates were obtained for models built with individual machine learning algorithms, depending on the algorithm used. Hybrid models, on the other hand, produced more consistent results. Among the individual machine learning algorithms, the highest determination coefficients were obtained with SA2, while the lowest values were obtained with SA4. Stable and similar results were obtained with hybrid models. As a result, establishing hybrid models instead of individual machine learning algorithms is very important for obtaining more stable results [31,41]. The machine learning algorithm with the highest coefficient of determination is CatBoost for one feature, random forest for two and three features, and a hybrid structure in which all algorithms are used for four and five features. In similar studies in the literature, coefficients of determination were found to be 0.88–0.93 for CatBoost [50], 0.86 for AdaBoost [51], and 0.47–0.74 for random forest [52]. The results agree with the current study, and higher coefficients of determination were obtained for some algorithms.

Tables 12–16 shows the performance evaluation metrics of the models built with the most successful datasets according to the number of features. The biggest coefficient of determination was obtained with SA1 for one feature, SA2 for two and three features, and HA7, which is a hybrid structure, for four and five features. The most unsuccessful models were obtained with the single-structure SA4. The lowest MAPE values for models with one, two, three, four, and five features were 11.61, 11.03, 10.05, 9.2, and 9.62, respectively. As the number of features in the established models rose, the MAPE value decreased, but when all characteristics were employed, it increased slightly [31].

Fig. 15 presents a graphical analysis of the most successful models for high-performance datasets. As the number of input features increased, the models' performance improved. However, a slight decline in performance was observed when all five features were used. Among the models built with single and hybrid algorithms, the highest performance was achieved by the hybrid model with four input features. Including the fifth feature led to a minor reduction in prediction accuracy. Performance metrics revealed that the optimal number of input features was four for the SA1 algorithm and three for the SA2 algorithm. In all models, the R^2 values exceeded 0.95, indicating excellent predictive performance. A comparison of multiple performance metrics confirmed the consistency of these results. It can be concluded that hybrid models offer more stable and generalizable predictions than individual models. Additionally, incorporating input features with a strong correlation to the output response enhances model performance [31]. Nevertheless, combinations of features with lower correlations can also be successfully utilized to develop more accurate machine learning models.

Fig. 16 illustrates the relationship between test models and the number of input features. While models built with only one feature exhibit lower accuracy, their predictive performance significantly improves as the number of features increases. The actual values and forecast results in this study demonstrate a strong alignment, indicating the robustness of the models. Among the models tested, the hybrid model HA7 provided the most balanced and consistent predictions. Due to its high reliability in modeling and accurately predicting feed force during boring operations, the HA7 model is recommended for precise forecasting. This enables efficient process planning by allowing the feed force to be accurately predicted before machining. Additionally, the proposed approach serves as an indirect measurement model, offering a more practical and cost-effective alternative to expensive and complex dynamometers, further enhancing its applicability in industrial settings.

To sum up, when the created datasets and established models are

Table 10
All features and models obtained by PCA.

R^2		Established machine learning models										
Datasets	**Features**	**SA1**	**SA2**	**SA3**	**SA4**	**HA1**	**HA2**	**HA3**	**HA4**	**HA5**	**HA6**	**HA7**
31	All (5)	0.978	0.988	0.964	0.899	0.992	0.985	0.964	0.978	0.983	0.989	**0.994**
32	PCA	0.820	0.821	0.844	0.840	0.820	0.833	0.833	0.833	0.833	**0.844**	0.834

Bold: The test datasets' most significant coefficients of determination.

Table 11
The most successful models by number of features.

R^2		Established machine learning models										
Datasets	**Features**	**SA1**	**SA2**	**SA3**	**SA4**	**HA1**	**HA2**	**HA3**	**HA4**	**HA5**	**HA6**	**HA7**
5	DOC	**0.973**	0.971	0.942	0.889	0.972	0.960	0.943	0.958	0.941	0.924	0.952
14	CS-DOC	0.958	**0.990**	0.961	0.898	0.978	0.960	0.982	0.980	0.975	0.986	0.989
19	CT-CS-FR	0.968	**0.993**	0.962	0.898	0.987	0.975	0.970	0.984	0.972	0.988	0.991
30	IR-CS-FR-DOC	0.985	0.989	0.964	0.899	0.992	0.984	0.970	0.979	0.982	0.990	**0.995**
31	All (5)	0.978	0.988	0.964	0.899	0.992	0.985	0.964	0.978	0.983	0.989	**0.994**

Bold: The datasets' most significant coefficients of determination.

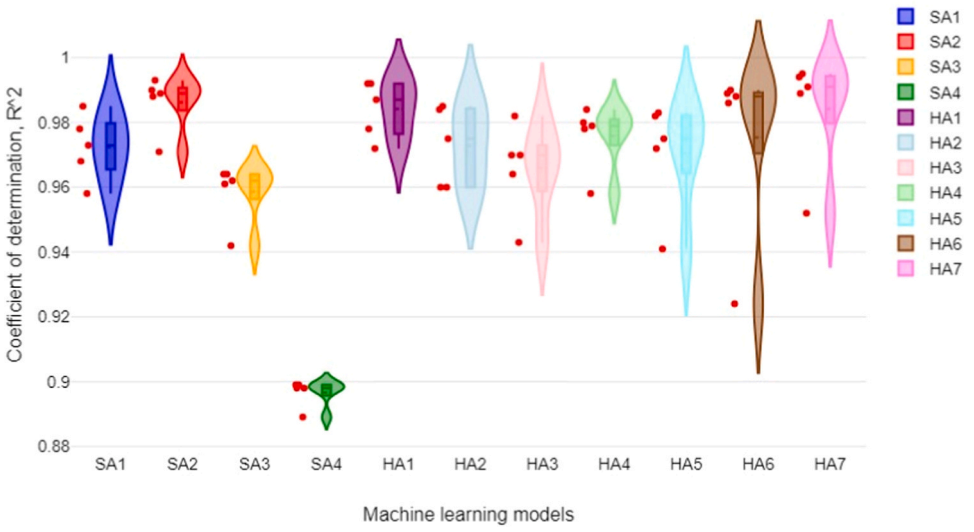


Fig. 14. Coefficients of determination obtained with the most successful models.

Table 12
Comparison of models built with the DOC feature.

Features = DOC		**Performance evaluation metrics**					
Symbol	**Models**	**MAPE**	**RMSE**	**MAE**	**SH**	**R^2**	**MSE**
SA1	CB	11.61	9.42	6.81	12.75	0.973	88.71
SA2	RF	11.81	9.82	6.98	13.30	0.971	96.52
SA3	AB	15.30	13.72	9.75	18.58	0.942	188.23
SA4	RR	30.95	19.07	15.97	25.82	0.889	363.56
HA1	CB+RF	11.71	9.62	6.89	13.03	0.972	92.55
HA2	CB+AB	13.29	11.50	8.17	15.57	0.960	132.16
HA3	CB+RR	19.12	13.72	10.53	18.58	0.943	188.22
HA4	RF+AB	13.50	11.72	8.33	15.86	0.958	137.26
HA5	RF+RR	19.31	13.94	10.68	18.87	0.941	194.22
HA6	AB+RR	20.44	15.82	11.88	21.42	0.924	250.16
HA7	CB+RF+AB+RR	15.06	12.51	9.00	16.94	0.952	156.52

Table 13
Comparison of models built with the CS-DOC combination.

Features = CS-DOC		**Performance evaluation metrics**					
Symbol	**Models**	**MAPE**	**RMSE**	**MAE**	**SH**	**R^2**	**MSE**
SA1	CB	18.19	11.73	9.64	15.88	0.958	137.52
SA2	RF	11.03	5.61	4.98	7.59	0.990	31.46
SA3	AB	14.36	11.34	8.47	15.35	0.961	128.52
SA4	RR	29.70	18.30	15.31	24.78	0.898	334.91
HA1	CB+RF	14.61	8.40	7.31	11.38	0.978	70.58
HA2	CB+AB	16.03	11.47	8.96	15.53	0.960	131.59
HA3	CB+RR	15.99	7.62	6.51	10.31	0.982	58.01
HA4	RF+AB	12.45	8.11	6.63	10.98	0.980	65.76
HA5	RF+RR	17.01	9.12	8.05	12.35	0.975	83.17
HA6	AB+RR	13.55	6.69	5.70	9.05	0.986	44.71
HA7	CB+RF+AB+RR	12.23	5.87	5.04	7.94	0.989	34.40

Table 14
Comparison of models established with the combination of CT-CS-FR.

Features = CT-CS-FR		Performance evaluation metrics					
Symbol	**Models**	**MAPE**	**RMSE**	**MAE**	**SH**	**R^2**	**MSE**
SA1	CB	15.72	10.27	8.28	13.91	0.968	105.57
SA2	RF	10.05	4.70	4.19	6.36	0.993	22.05
SA3	AB	14.01	11.20	8.12	15.16	0.962	125.44
SA4	RR	29.85	18.28	15.36	24.75	0.898	334.07
HA1	CB+RF	12.21	6.43	5.67	8.71	0.987	41.40
HA2	CB+AB	13.12	9.08	6.82	12.29	0.975	82.37
HA3	CB+RR	17.05	9.83	7.76	13.31	0.970	96.66
HA4	RF+AB	11.70	7.24	5.95	9.80	0.984	52.41
HA5	RF+RR	17.10	9.59	8.24	12.99	0.972	92.03
HA6	AB+RR	13.58	6.36	5.57	8.61	0.988	40.46
HA7	CB+RF+AB+RR	11.31	5.29	4.44	7.16	0.991	27.94

Table 15
Comparison of models built with the combination of IR-CS-FR-DOC.

Features = IR-CS-FR-DOC		Performance evaluation metrics					
Symbol	**Models**	**MAPE**	**RMSE**	**MAE**	**SH**	**R^2**	**MSE**
SA1	CB	12.10	7.10	5.16	9.62	0.985	50.44
SA2	RF	9.73	6.11	5.04	8.27	0.989	37.32
SA3	AB	11.55	10.79	7.43	14.60	0.964	116.32
SA4	RR	29.71	18.22	15.26	24.68	0.899	332.11
HA1	CB+RF	9.92	5.24	4.34	7.09	0.992	27.44
HA2	CB+AB	10.63	7.17	5.47	9.71	0.984	51.38
HA3	CB+RR	18.94	9.94	8.63	13.46	0.970	98.82
HA4	RF+AB	10.54	8.29	6.20	11.23	0.979	68.76
HA5	RF+RR	15.02	7.70	6.84	10.42	0.982	59.28
HA6	AB+RR	12.60	5.80	5.14	7.86	0.990	33.67
HA7	CB+RF+AB+RR	9.20	4.22	3.22	5.71	0.995	17.81

Table 16
Comparison of established models with all features.

Features = All (5)		Performance evaluation metrics					
Symbol	**Models**	**MAPE**	**RMSE**	**MAE**	**SH**	**R^2**	**MSE**
SA1	CB	13.42	8.49	6.37	11.49	0.978	72.04
SA2	RF	9.23	6.17	5.00	8.36	0.988	38.11
SA3	AB	12.07	10.85	7.61	14.70	0.964	117.81
SA4	RR	29.87	18.20	15.31	24.64	0.899	331.09
HA1	CB+RF	9.26	5.19	4.14	7.03	0.992	26.98
HA2	CB+AB	10.27	6.91	5.09	9.35	0.985	47.71
HA3	CB+RR	19.81	10.84	9.21	14.67	0.964	117.42
HA4	RF+AB	10.65	8.40	6.30	11.38	0.978	70.60
HA5	RF+RR	14.78	7.51	6.71	10.16	0.983	56.35
HA6	AB+RR	12.82	5.91	5.21	8.00	0.989	34.88
HA7	CB+RF+AB+RR	9.62	4.31	3.54	5.84	0.994	18.60

compared, the highest coefficient of determination value was calculated as 0.995 with the hybrid structure HA7 established with the IR-CS-FR-DOC feature combination in dataset number 30. The highest coefficients of determination, models, and MAPE values for feature numbers 1, 2, 3, 4, and 5, respectively, are 0.973/SA1/11.61, 0.99/SA2/11.03, 0.993/SA2/10.05, 0.995/HA7/9.2, and 0.994/HA7/9.62. With simple regression equations, the coefficient of determination for the DOC feature was calculated as 0.77, for CS-DOC features as 0.81, for CT-CS-FR features as 0.04, for IR-CS-FR-DOC features as 0.82, and for all features as 0.83. According to the values obtained with simple regression equations, it is clear that the models established with the machine learning method give higher levels and much more successful results. According to performance evaluation criteria such as the coefficient of determination and MAPE, as the quantity of features rises, so does model success, although the success rate eventually declines. It has been determined that as the number of features increases, hybrid models built against individual models give more effective results. Models built with the help of feature combinations enabled the prediction of feed force with a high success rate.

4. Conclusion

This work aims to apply machine learning approaches to determine the feed force that occurs during the boring process of AISI P20 plastic mold steel using a precision boring bar, as well as to determine the best input feature combinations and datasets. As a result of the study, the most optimum input feature combinations can be determined to predict the feed force with high success. When the proposed method is used, it will be possible to eliminate the dynamometer cost, reduce the measurement cost, save time, shorten the machine adjustment time, achieve effective process planning, and increase efficiency.

The most successful model established with one input feature was the DOC feature and SA1 model with an R^2 value of 0.973, while the most successful model for two input features was the CS-DOC combination and SA2 model with an R^2 value of 0.99. For three input features, an R^2 value of 0.993 was obtained with CT-CS-FR and CT-CS-DOC

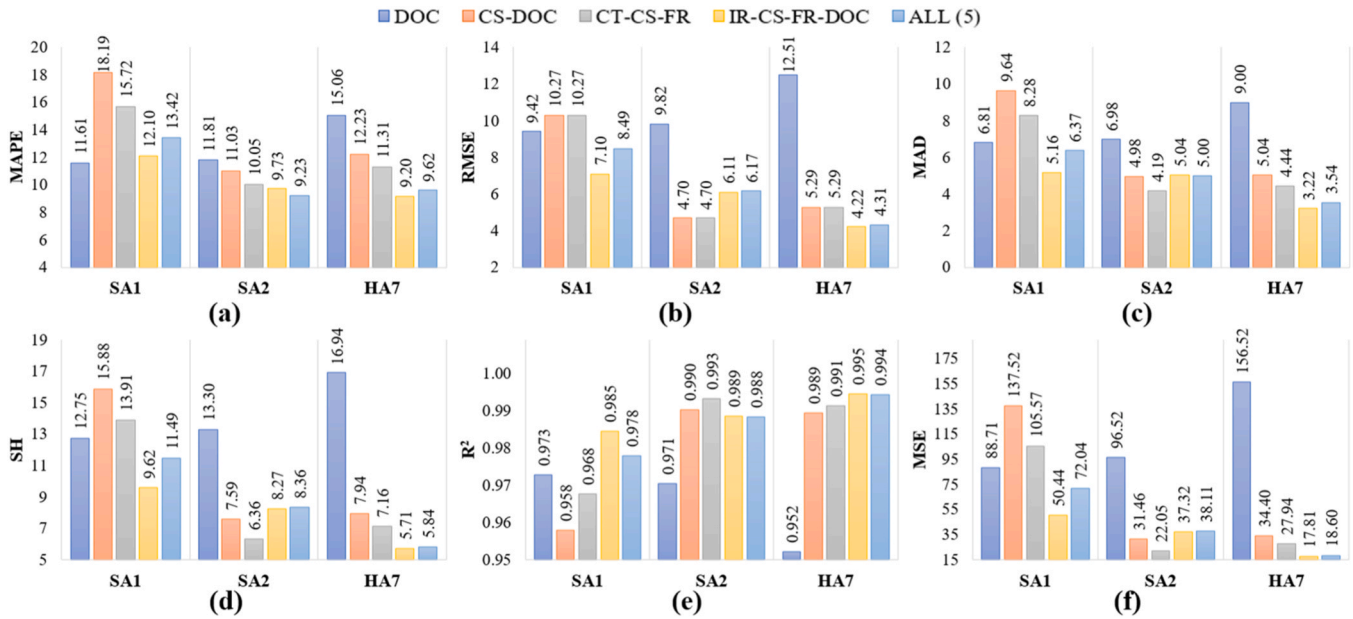


Fig. 15. Model comparison graphs for high-performing datasets **(a)** MAPE, **(b)** RMSE, **(c)** MAD, **(d)** SH, **(e)** R^2, **(f)** MSE.

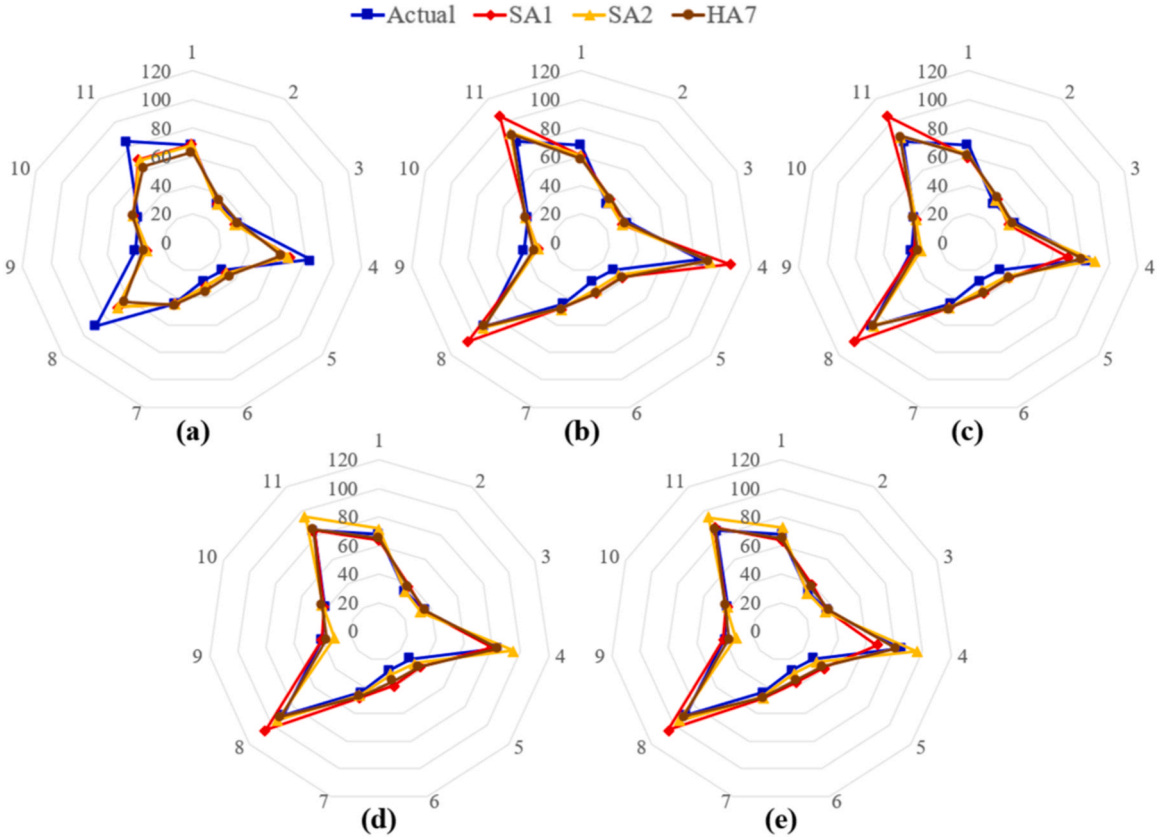


Fig. 16. Comparison of test models according to the number of features **(a)** DOC, **(b)** CS-DOC, **(c)** CT-CS-FR, **(d)** IR-CS-FR-DOC, **(e)** ALL (5).

combinations and the SA2 model, while for four input features, an R^2 value of 0.995 was obtained with the IR-CS-FR-DOC combination and the HA7 model. When all input features were used, the R^2 value was calculated as 0.994 with the HA7 model. PCA showed lower performance compared to other models, and the R^2 value was calculated as 0.844 with the HA6 model. While individual models are more successful when the number of features in the dataset is smaller, it can be said that hybrid models give more consistent and stable results as the number of features rises. As the number of features rises, the prediction error according to performance evaluation metrics tends to decrease, but it increases slightly when all data is used. Although more successful models were established with features with high Pearson correlation coefficients, highly successful models could also be established with some combinations of features with lower coefficients. Therefore, comparing

many feature combinations and using many ML algorithms is very necessary for models with high success rates. The success of the models varied according to the quantity of features in the dataset. However, the coefficients of determination for all models were within acceptable ranges. To summarize, feed force may be accurately forecast by employing machine learning techniques and feature combinations collected from boring parameters.

5. Future works

The purpose of this study was to predict the boring feed force with a high success rate in precision boring holes in AISI P20 plastic mold steel utilizing the most effective input feature combination and machine learning techniques. This study's scope can be expanded with extra information. Future work can be classified into the following categories:

- Features can be obtained for workpiece categories beyond plastic mold steel AISI P20.
- Various algorithms can be used to build models.
- Various combinations of dataset features can be employed.
- ML algorithms can accurately predict output reactions like tool life, dimensional accuracy, and surface roughness.

Declaration of Competing Interest

The authors declare that they have no known competing financial interests or personal relationships that could have appeared to influence the work reported in this paper.

Acknowledgements

The Gazi University's Scientific Research Projects Unit provided funding under grant number 07/2011–70 for this project. The researchers appreciate the assistance provided by Gazi University's BAP department.

Data Availability

Data will be made available on request.

References

[1] J.-Y. Chen, K. Conlon, L. Xue, R. Rogge, Experimental study of residual stresses in laser clad AISI P20 tool steel on pre-hardened wrought P20 substrate, Mater. Sci. Eng.: A 527 (2010) 7265–7273, https://doi.org/10.1016/j.msea.2010.07.098.
[2] F. Shiou, C. Cheng, Ultra-precision surface finish of NAK80 mould tool steel using sequential ball burnishing and ball polishing processes, J. Mater. Process. Technol. 201 (2008) 554–559, https://doi.org/10.1016/j.jmatprotec.2007.11.235.
[3] D. Mathivanan, M. Nouby, R. Vidhya, Minimization of sink mark defects in injection molding process–Taguchi approach, Int. J. Eng., Sci. Technol. 2 (2010) 13–22, https://doi.org/10.4314/ijest.v2i2.59133.
[4] J.C. Milan, A.R. Machado, Í.V. Tomaz, L.R. da Silva, C.A. Barbosa, M. Mia, D. Y. Pimenov, Effects of calcium-treatment of a plastic injection mold steel on the tool wear and power consumption in slot milling, J. Mater. Res. Technol. 13 (2021) 1103–1114, https://doi.org/10.1016/j.jmrt.2021.05.021.
[5] N.A. Özbek, O. Özbek, F. Kara, Statistical analysis of the effect of the cutting tool coating type on sustainable machining parameters, J. Mater. Eng. Perform. 30 (2021) 7783–7795, https://doi.org/10.1007/s11665-021-06066-8.
[6] R.P. Zeilmann, G.L. Nicola, T. Vacaro, C.R. Teixeira, R. Heiler, Implications of the reduction of cutting fluid in drilling AISI P20 steel with carbide tools, Int. J. Adv. Manuf. Technol. 58 (2012) 431–441, https://doi.org/10.1007/s00170-011-3401-8.
[7] T.F.L. Melo, S.L.M. Ribeiro Filho, É.M. Arruda, L.C. Brandão, Analysis of the surface roughness, cutting efforts, and form errors in bore reaming of hardened steel using a statistical approach, Measurement 134 (2019) 845–854, https://doi.org/10.1016/j.measurement.2018.12.033.
[8] A. Parsian, Stability Prediction of Multiple-Teeth Boring Operations (Master's thesis), Department of Mechanical Engineering, Blekinge Institute of Technology, Karlskrona, Sweden, 2013.
[9] M. Slamani, R. Mayer, M. Balazinski, S. Engin, Identification and compensation of dynamic scale mismatches in high-speed end mill boring trajectory on CNC machines, (2010) ⟨https://doi.org/10.1115/1.4001412⟩.
[10] A. Del Taglia, G. Tani, A method for measuring cutting forces in boring operations, Int. J. Mach. Tool. Des. Res. 22 (1982) 23–30, https://doi.org/10.1016/0020-7357(82)90017-8.
[11] I. Lazoglu, F. Atabey, Y. Altintas, Dynamics of boring processes: Part III-time domain modeling, Int. J. Mach. Tools Manuf. 42 (2002) 1567–1576, https://doi.org/10.1016/S0890-6955(02)00067-6.
[12] H.B. Lacerda, I.L. Siqueira, Blade geometry effects on the boring of valve seats of internal combustion engines, Int. J. Adv. Manuf. Technol. 63 (2012) 269–280, https://doi.org/10.1007/s00170-012-3905-x.
[13] M. Arsuaga, L.L. de Lacalle, R. Lobato, G. Urbikain, F. Campa, Effect of centrifugal forces on dimensional error of bored shapes. AIP Conference Proceedings, American Institute of Physics, 2012, https://doi.org/10.1063/1.4707624.
[14] F. Valdivielso, Instrumentation and control methodology for zero defect manufacturing in boring operations, Ann. DAAAM Proc. 23 (2012).
[15] E. Budak, E. Ozlu, Analytical modeling of chatter stability in turning and boring operations: a multi-dimensional approach, CIRP Ann. 56 (2007) 401–404, https://doi.org/10.1016/j.cirp.2007.05.093.
[16] G. Subramani, S. Kapoor, R. DeVor, A model for the prediction of bore cylindricity during machining, (1993) ⟨https://doi.org/10.1115/1.2901630⟩.
[17] M. Günay, T. Meral, Modelling and multiresponse optimization for minimizing burr height, thrust force and surface roughness in drilling of ferritic stainless steel, Sādhanā 45 (2020) 273, https://doi.org/10.1007/s12046-020-01490-3.
[18] Q. Liu, D. Gao, R. Jia, Q. Zhou, Z. Bai, Investigating the cutting force monitoring system in the boring process, Int. J. Adv. Manuf. Technol. (2022) 1–13, https://doi.org/10.1007/s00170-021-08451-y.
[19] F. Atabey, I. Lazoglu, Y. Altintas, Mechanics of boring processes—Part I, Int. J. Mach. Tools Manuf. 43 (2003) 463–476, https://doi.org/10.1016/S0890-6955(02)00276-6.
[20] F. Atabey, I. Lazoglu, Y. Altintas, Mechanics of boring processes—Part II—multi-insert boring heads, Int. J. Mach. Tools Manuf. 43 (2003) 477–484, https://doi.org/10.1016/S0890-6955(02)00277-8.
[21] N. Yussefian, B. Moetakef-Imani, H. El-Mounayri, The prediction of cutting force for boring process, Int. J. Mach. Tools Manuf. 48 (2008) 1387–1394, https://doi.org/10.1016/j.ijmachtools.2008.05.003.
[22] B. Moetakef-Imani, N. Yussefian, Dynamic simulation of boring process, Int. J. Mach. Tools Manuf. 49 (2009) 1096–1103, https://doi.org/10.1016/j.ijmachtools.2009.07.008.
[23] H. Cheng, J. Zhao, R. Sun, S. Liu, Z. Yang, Finish boring process of hard alloy cutter based on electrostatic cooling-aided machining, Int. J. Adv. Manuf. Technol. 111 (2020) 2999–3013, https://doi.org/10.1007/s00170-020-06298-3.
[24] M.K. Uçar, K. Uçar, Z. Ucar, M.R. Bozkurt, Determination gender-based hybrid artificial intelligence of body muscle percentage by photoplethysmography signal, Comput. Methods Prog. Biomed. 224 (2022) 107010, https://doi.org/10.1016/j.cmpb.2022.107010.
[25] P. Charalampous, Prediction of cutting forces in milling using machine learning algorithms and finite element analysis, J. Mater. Eng. Perform. 30 (2021) 2002–2013, https://doi.org/10.1007/s11665-021-05507-8.
[26] V. Dubey, A.K. Sharma, H. Kumar, P.K. Arora, Prediction of cutting forces in MQL turning of AISI 304 STeel using machine learning algorithm, J. Eng. Res. (2022) 1–13, https://doi.org/10.36909/jer.ICMET.17177.
[27] S. Wan, X. Li, Y. Yin, J. Hong, Milling chatter detection by multi-feature fusion and Adaboost-SVM, Mech. Syst. Signal Process. 156 (2021) 107671, https://doi.org/10.1016/j.ymssp.2021.107671.
[28] T. Banda, Y.-c Liu, A.A. Farid, C.S. Lim, A machine learning model for flank wear prediction in face milling of Inconel 718, Int. J. Adv. Manuf. Technol. 126 (2023) 935–945, https://doi.org/10.1007/s00170-023-11152-3.
[29] S. Vijay, B. Kuraichen, Data Driven Prognostics of Milling Tool Wear: A Machine Learning Approach. 2021 International Conference on Computational Performance Evaluation (ComPE), IEEE, 2021, https://doi.org/10.1109/ComPE53109.2021.9751990.
[30] M.K. Uçar, Z. Ucar, K. Uçar, M. Akman, M.R. Bozkurt, Determination of body fat percentage by electrocardiography signal with gender based artificial intelligence, Biomed. Signal Process. Control 68 (2021) 102650, https://doi.org/10.1016/j.bspc.2021.102650.
[31] M.K. Uçar, Z. Ucar, F. Köksal, N. Daldal, Estimation of body fat percentage using hybrid machine learning algorithms, Measurement 167 (2021) 108173, https://doi.org/10.1016/j.measurement.2020.108173.
[32] Y. Wang, X. Huang, X. Ren, Z. Chai, X. Chen, In-process belt-image-based material removal rate monitoring for abrasive belt grinding using CatBoost algorithm, Int. J. Adv. Manuf. Technol. 123 (2022) 2575–2591, https://doi.org/10.1007/s00170-022-10341-w.
[33] S.H. Trinh, H.-B. Ly, Enhancing Compressive Strength Prediction of Roller Compacted Concrete Using Machine Learning Techniques, Measurement (2023) 113196, https://doi.org/10.1016/j.measurement.2023.113196.
[34] L. Breiman, Random forests, Mach. Learn. 45 (2001) 5–32, https://doi.org/10.1023/A:1010933404324.
[35] Y. Freund, R.E. Schapire, Experiments with a new boosting algorithm. Machine Learning: Proceedings of the Thirteenth International Conference, Citeseer, 1996.
[36] M.K. Gupta, M.E. Korkmaz, H. Yılmaz, Ş. Şirin, N.S. Ross, M. Jamil, G.M. Królczyk, V.S. Sharma, Real-time monitoring and measurement of energy characteristics in sustainable machining of titanium alloys, Measurement (2023) 113937, https://doi.org/10.1016/j.measurement.2023.113937.
[37] R. Agarwal, J. Singh, V. Gupta, An intelligent approach to predict thermal injuries during orthopaedic bone drilling using machine learning, J. Braz. Soc. Mech. Sci. Eng. 44 (2022) 320, https://doi.org/10.1007/s40430-022-03630-8.

[38] J.T. Vieira, R.B.D. Pereira, C.H. Lauro, L.C. Brandão, J.R. Ferreira, Multi-objective evolutionary optimization of extreme gradient boosting regression models of the internal turning of PEEK tubes, Expert Syst. Appl. 238 (2024) 122372, https://doi.org/10.1016/j.eswa.2023.122372.
[39] I. Moran, D.T. Altilar, M.K. Ucar, C. Bilgin, M.R. Bozkurt, Deep transfer learning for chronic obstructive pulmonary disease detection utilizing electrocardiogram signals, IEEE Access (2023), https://doi.org/10.1109/ACCESS.2023.3269397.
[40] Z. Li, J. Zhang, B. Dai, Y. Liu, Microstructure and corrosion resistance property of laser transformation hardening pre-hardened AISI P20 plastic die steel, Opt. Laser Technol. 122 (2020) 105852, https://doi.org/10.1016/j.optlastec.2019.105852.
[41] A. Akdulum, Y. Kayir, Prediction of thrust force in indexable drilling of aluminum alloys with machine learning algorithms, Measurement 222 (2023) 113655, https://doi.org/10.1016/j.measurement.2023.113655.
[42] A. Akdulum, Y. Kayir, Investigation of the effect of u drills with different properties on thrust force, torque and spindle load, Politek. Derg. 26 (2023) 387–400, https://doi.org/10.2339/politeknik.1113301.
[43] A. Akdulum, Y. Kayir, Experimental investigation and optimization of process stability in drilling of Al 7075-T651 using indexable insert drills, J. Braz. Soc. Mech. Sci. Eng. 45 (2023) 429, https://doi.org/10.1007/s40430-023-04303-w.
[44] O. Keblouti, L. Boulanouar, M.W. Azizi, M.A. Yallese, Effects of coating material and cutting parameters on the surface roughness and cutting forces in dry turning of AISI 52100 steel, Struct. Eng. Mech., Int'l J. 61 (2017) 519–526, https://doi.org/10.12989/sem.2017.61.4.519.
[45] Y. Erkoçak, Y. Kayır, Analyzing the impacts of cutting parameters on cutting forces in the taguchi method for boring high-alloy white cast irons with CBN inserts, Arab. J. Sci. Eng. 48 (2023) 12569–12585, https://doi.org/10.1007/s13369-023-08008-z.
[46] A. Ebrahimi, M. Moshksar, Study of machinability in boring operation of microalloyed and heat-treated alloy steels, Mater. Sci. Eng.: A 460 (2007) 314–323, https://doi.org/10.1016/j.msea.2007.01.050.
[47] G. Xu, X. Wang, Support vector regression optimized by black widow optimization algorithm combining with feature selection by MARS for mining blast vibration prediction, Measurement (2023) 113106, https://doi.org/10.1016/j.measurement.2023.113106.
[48] B. Li, T. Liu, J. Liao, C. Feng, L. Yao, J. Zhang, Non-invasive milling force monitoring through spindle vibration with LSTM and DNN in CNC machine tools, Measurement 210 (2023) 112554, https://doi.org/10.1016/j.measurement.2023.112554.
[49] W. Zhang, L. Zhang, J. Yang, X. Hao, G. Guan, Z. Gao, An experimental modeling of cyclone separator efficiency with PCA-PSO-SVR algorithm, Powder Technol. 347 (2019) 114–124, https://doi.org/10.1016/j.powtec.2019.01.070.
[50] S.M. Najm, T. Trzepieciński, M. Kowalik, Modelling and parameter identification of coefficient of friction for deep-drawing quality steel sheets using the CatBoost machine learning algorithm and neural networks, Int. J. Adv. Manuf. Technol. 124 (2023) 2229–2259, https://doi.org/10.1007/s00170-022-10544-1.
[51] M. Cheng, L. Jiao, P. Yan, L. Feng, T. Qiu, X. Wang, B. Zhang, Prediction of surface residual stress in end milling with Gaussian process regression, Measurement 178 (2021) 109333, https://doi.org/10.1016/j.measurement.2021.109333.
[52] Y.J. Cruz, M. Rivas, R. Quiza, R.E. Haber, F. Castaño, A. Villalonga, A two-step machine learning approach for dynamic model selection: a case study on a micro milling process, Comput. Ind. 143 (2022) 103764, https://doi.org/10.1016/j.compind.2022.103764.